

Testing backreaction effects with observational Hubble parameter data

Shu-Lei Cao,^a Huan-Yu Teng,^a Hao-Ran Yu^b Hao-Yi Wan^{a,c} and Tong-Jie Zhang^{a,d,1}

^aDepartment of Astronomy, Beijing Normal University, Beijing, 100875, China

^bKavli Institute for Astronomy & Astrophysics, Peking University, Beijing, 100871, China

^cNational Astronomical Observatories, Chinese Academy of Sciences, Beijing 100012, China

^dSchool of Information Management, School of Physics and Electric Information, Shandong Provincial Key Laboratory of Biophysics, Dezhou University, Dezhou 253023, China

E-mail: slcao@mail.bnu.edu.cn, tjzhang@bnu.edu.cn

Abstract. The spatially averaged inhomogeneous Universe includes a kinematical backreaction term $\mathcal{Q}_{\mathcal{D}}$ that is related to the averaged spatial Ricci scalar $\langle \mathcal{R} \rangle_{\mathcal{D}}$ in the framework of general relativity. Under the assumption that $\mathcal{Q}_{\mathcal{D}}$ and $\langle \mathcal{R} \rangle_{\mathcal{D}}$ obey the scaling laws of the volume scale factor $a_{\mathcal{D}}$, a direct coupling between them with a scaling index n is remarkable. In order to explore the generic properties of a backreaction model to explain the observations of the Universe, we exploit two metrics to describe the late time Universe. Since the standard FLRW metric cannot precisely describe the late time Universe on small scales, the template metric with an evolving curvature parameter is employed. However, we doubt that the evolving curvature parameter also obeys the scaling law, thus we make use of observational Hubble parameter data (OHD) to constrain parameters in dust cosmology to testify it. First, in FLRW model, after getting best-fit constraints of $\Omega_m^{\mathcal{D}_0} = 0.25_{-0.03}^{+0.03}$, $n = 0.02_{-0.66}^{+0.69}$, and $H_{\mathcal{D}_0} = 70.54_{-3.97}^{+4.24}$ km/s/Mpc, evolutions of parameters are studied. Second, in template metric context, by marginalizing over $H_{\mathcal{D}_0}$ as a prior of uniform distribution, we obtain the best-fit values as $n = -1.22_{-0.41}^{+0.68}$ and $\Omega_m^{\mathcal{D}_0} = 0.12_{-0.02}^{+0.04}$. Moreover, we utilize three different Gaussian priors of $H_{\mathcal{D}_0}$, which result in different best-fits of n , but almost the same best-fit value of $\Omega_m^{\mathcal{D}_0} \sim 0.12$. With these constraints, evolutions of the effective deceleration parameter $q^{\mathcal{D}}$ indicate that the backreaction can account for the accelerated expansion of the Universe without involving extra dark energy component in the scaling solution context. However, the results also imply that the prescription of the geometrical instantaneous spatially-constant curvature $\kappa_{\mathcal{D}}$ of the template metric is insufficient and should be improved.

¹Corresponding author.

Contents

1	Introduction	1
2	The backreaction model	2
3	Effective geometry	4
3.1	The template metric	4
3.2	Computation of Observables	5
4	Constraints with OHD	6
4.1	The flat FLRW model	6
4.2	The template metric model	9
4.3	Testing the effective deceleration parameter	12
5	Conclusions and discussions	13

1 Introduction

The universe is homogeneous and isotropic on very large scales. According to Einstein's general relativity, one can obtain a homogeneous and isotropic solution of Einstein's field equations, which is called Friedmann-Lemaitre-Robertson-Walker (FLRW) metric. Since on smaller scales the universe appears to be strongly inhomogeneous and anisotropic, Larena et al. [1] doubt that the FLRW cosmology describes the averaged inhomogeneous universe at all times. They assume that FLRW metric may not hold at late times especially when there are large matter inhomogeneities existed, even though it may be suitable at early times. Therefore they introduce a template metric that is compatible with homogeneity and isotropy on large scales of FLRW cosmology, and also contains structuring on small scales. In other words, this metric is built upon weak, instead of strong, cosmological principle.

The observations of type Ia supernovae (SNe Ia) [2, 3] suggest that the universe is in a state of accelerated expansion, which implies that there exists a latent component so called Dark Energy with quality of negative pressure that operates the accelerated expansion of the universe. There are many scenarios proposed to account for the observations. The simplest one is the positive cosmological constant in Einstein's equations, which in common assumption is equivalent to the quantum vacuum. Since the measured cosmological constant is much smaller than the particle physics predicted, some other scenarios are proposed, such as the phenomenological models which explained Dark Energy as a late time slow rolling scalar field [4] or the Chaplygin gas [5], and the modified gravity models. Recently, a new scenario [6, 7] is raised to consider dark energy as a backreaction effect of inhomogeneities on the average expansion of the universe. Here we specifically focus on the backreaction model without involving perturbation theory.

According to Buchert [8], averaged equations of the averaged spatial Ricci scalar $\langle \mathcal{R} \rangle_{\mathcal{D}}$ and the 'backreaction' term $\mathcal{Q}_{\mathcal{D}}$ can be solved to obtain the exact scaling solutions in which a direct coupling between $\langle \mathcal{R} \rangle_{\mathcal{D}}$ and $\mathcal{Q}_{\mathcal{D}}$ with a scaling index n is significant. With that solution, a domain-dependent Hubble function (effective volume Hubble parameter) $H_{\mathcal{D}}$ can be expressed with the scaling index n and the present effective matter density parameter

$\Omega_m^{\mathcal{D}_0}$. Also, as mentioned in [1], the pure scaling ansatz is not what we expected in a realistic evolution of backreaction.

In order to explore the generic properties of a backreaction model to explain the observations of the Universe, we, in this paper, exploit two metrics to describe the late time Universe. Although the template metric proposed by Larena et. al. [1] is reasonable, the prescription of the so-called ‘‘geometrical instantaneous spatially-constant curvature’’ $\kappa_{\mathcal{D}}$ is skeptical, based on the discrepancies between our results and theirs. Comparing the FLRW metric with the smoothed template metric, we use observational Hubble parameter data (OHD) to constrain the scaling index n (corresponding to constant equation of state for morphon field $w_{\Phi}^{\mathcal{D}}$ [9]) and the present effective matter density parameter $\Omega_m^{\mathcal{D}_0}$ without involving perturbation theory. In the latter case, according to [10], we choose to marginalize over both the top-hat prior of $H_{\mathcal{D}_0}$ with a uniform distribution in the interval [50, 90] and three different Gaussian priors of $H_{\mathcal{D}_0}$. Combining both the FLRW geometry and the template metric with the backreaction model, we obtain the fine relation between effective Hubble parameter $H_{\mathcal{D}}$ and effective scale factor $a_{\mathcal{D}}$, and utilize Runge-Kutta method to solve the differential equations of latter, in order to acquire the link between $a_{\mathcal{D}}$ and effective redshift $z_{\mathcal{D}}$. At last, a conflict, as expected, arises. Our results show that it needs a higher instead of lower amount of backreaction to interpret the effective geometry, even though accelerated expansion of $a_{\mathcal{D}}$ still remains. The power law prescription of $\kappa_{\mathcal{D}}$ certainly need to be improved, since it only evolves from 0 to -1, which is insufficient. Of course, we should point out that the power law ansatz is not the realistic case and the results are expected to be inaccurate. For simplicity, we only deliberate the situation under the assumption of power-law ansatz.

The paper is organized as follows. The backreaction context is demonstrated in Section 2. In Section 3, we introduce the template metric and computation of observables along with the effective Hubble parameter $H_{\mathcal{D}}$, and demonstrate how to relate effective redshift $z_{\mathcal{D}}$ to effective scale factor $a_{\mathcal{D}}$. We also refer to overall cosmic equation of state $w_{\text{eff}}^{\mathcal{D}}$ [9] and how it differs from constant equation of state w . In Section 4, according to the effective Hubble parameter, we apply OHD with both the FLRW metric and the template metric, and make use of Metropolis-Hastings algorithm of the Markov-Chain-Monte-Carlo (MCMC) method and mesh-grid method, respectively, to obtain the constraints of the parameters. In former case, we employ the best-fits to illustrate the evolutions of $q^{\mathcal{D}}$, $w_{\text{eff}}^{\mathcal{D}}$, $\kappa_{\mathcal{D}}$ and density parameters. In latter case, we test the effective deceleration parameter with the best-fit values. After analysis of the results in Section 4, we summarize our conclusion and discussion in Section 5.

We apply the natural units $c = 1$ everywhere, and assign that Greek indices such as α , μ run through 0...3, while Latin indices such as i, j run through 1...3.

2 The bacreaction model

Buchert [8] introduced a model of dust cosmologies, which leads to two averaged equations that we need, the averaged Raychaudhuri equation

$$3\frac{\ddot{a}_{\mathcal{D}}}{a_{\mathcal{D}}} + 4\pi G\langle\rho\rangle_{\mathcal{D}} - \Lambda = \mathcal{Q}_{\mathcal{D}} ; \quad (2.1)$$

and the averaged Hamiltonian constraint

$$3\left(\frac{\dot{a}_{\mathcal{D}}}{a_{\mathcal{D}}}\right)^2 - 8\pi G\langle\rho\rangle_{\mathcal{D}} + \frac{1}{2}\langle\mathcal{R}\rangle_{\mathcal{D}} - \Lambda = -\frac{\mathcal{Q}_{\mathcal{D}}}{2} , \quad (2.2)$$

where $\langle \varrho \rangle_{\mathcal{D}}$, G , and Λ represent averaged matter density in the domain \mathcal{D} , gravitational constant, and cosmological constant, respectively. The over-dot represents partial derivative as to proper time t here after. A effective scale factor is introduced via volume (normalized by the volume of the initial domain $V_{\mathcal{D}_i}$),

$$a_{\mathcal{D}}(t) = \left(\frac{V_{\mathcal{D}}(t)}{V_{\mathcal{D}_i}} \right)^{1/3}. \quad (2.3)$$

The averaged spatial Ricci scalar $\langle \mathcal{R} \rangle_{\mathcal{D}}$ and the ‘backreaction’ $\mathcal{Q}_{\mathcal{D}}$ are domain-dependent constants, which are time-dependent functions. The ‘backreaction’ term is expressed as

$$\mathcal{Q}_{\mathcal{D}} = 2\langle \mathbf{II} \rangle_{\mathcal{D}} - \frac{2}{3}\langle \mathbf{I} \rangle_{\mathcal{D}}^2 = \frac{2}{3}\langle (\theta - \langle \theta \rangle_{\mathcal{D}})^2 \rangle_{\mathcal{D}} - 2\langle \sigma^2 \rangle_{\mathcal{D}}, \quad (2.4)$$

with two scalar invariants

$$\mathbf{I} = \Theta^l_l = \theta, \quad (2.5)$$

and

$$\mathbf{II} = \frac{1}{2}(\theta^2 - \Theta^l_k \Theta^k_l) = \frac{1}{3}\theta^2 - \sigma^2, \quad (2.6)$$

where Θ_{ij} is the expansion tensor, with the trace-free symmetric shear tensor σ_{ij} , the rate of shear $\sigma^2 = \frac{1}{2}\sigma^i_j \sigma^j_i$ and the expansion rate θ . Substituting Eq. (2.1) into Eq. (2.2), one can get

$$(a_{\mathcal{D}}^6 \mathcal{Q}_{\mathcal{D}})^{\bullet} + a_{\mathcal{D}}^4 (a_{\mathcal{D}}^2 \langle \mathcal{R} \rangle_{\mathcal{D}})^{\bullet} = 0, \quad (2.7)$$

where the dot over the parentheses represents partial derivative over time t , and the solutions are

$$\langle \mathcal{R} \rangle_{\mathcal{D}} = \langle \mathcal{R} \rangle_{\mathcal{D}_i} a_{\mathcal{D}}^n; \quad \mathcal{Q}_{\mathcal{D}} = \mathcal{Q}_{\mathcal{D}_i} a_{\mathcal{D}}^m, \quad (2.8)$$

where n and m are real numbers. There are two types of solutions to be considered as mentioned in [8]. The first type is that when $n = -2$ and $m = -6$, the solution is corresponding to a quasi-FLRW universe at late time, which means backreaction is negligible. The second type is a direct coupling between $\langle \mathcal{R} \rangle_{\mathcal{D}}$ and $\mathcal{Q}_{\mathcal{D}}$, which states that when $m = n$, the exact relations between them are

$$\langle \mathcal{R} \rangle_{\mathcal{D}} = \langle \mathcal{R} \rangle_{\mathcal{D}_i} a_{\mathcal{D}}^n, \quad (2.9)$$

and

$$\mathcal{Q}_{\mathcal{D}} = -\frac{n+2}{n+6} \langle \mathcal{R} \rangle_{\mathcal{D}_i} a_{\mathcal{D}}^n. \quad (2.10)$$

A domain-dependent Hubble function is defined to be $H_{\mathcal{D}} = \dot{a}_{\mathcal{D}}/a_{\mathcal{D}}$, and dimensionless (‘effective’) averaged cosmological parameters are also given by

$$\Omega_m^{\mathcal{D}} = \frac{8\pi G \langle \varrho \rangle_{\mathcal{D}}}{3H_{\mathcal{D}}^2}, \quad (2.11)$$

$$\Omega_{\Lambda}^{\mathcal{D}} = \frac{\Lambda}{3H_{\mathcal{D}}^2}, \quad (2.12)$$

$$\Omega_{\mathcal{R}}^{\mathcal{D}} = -\frac{\langle \mathcal{R} \rangle_{\mathcal{D}}}{6H_{\mathcal{D}}^2}, \quad (2.13)$$

and

$$\Omega_{\mathcal{Q}}^{\mathcal{D}} = -\frac{\mathcal{Q}_{\mathcal{D}}}{6H_{\mathcal{D}}^2}. \quad (2.14)$$

Thus, according to Eq. (2.2), one can have

$$\Omega_m^{\mathcal{D}} + \Omega_\Lambda^{\mathcal{D}} + \Omega_{\mathcal{R}}^{\mathcal{D}} + \Omega_{\mathcal{Q}}^{\mathcal{D}} = 1 . \quad (2.15)$$

The components that are not included in Friedmann equation read

$$\Omega_X^{\mathcal{D}} = \Omega_{\mathcal{R}}^{\mathcal{D}} + \Omega_{\mathcal{Q}}^{\mathcal{D}} . \quad (2.16)$$

If $\Omega_\Lambda^{\mathcal{D}} = 0$, then $\Omega_X^{\mathcal{D}}$ is considered to be the Dark Energy contribution, and usually dubbed X-matter. By considering Eq. (2.9) and Eq. (2.10), one can get

$$\Omega_X^{\mathcal{D}} = -\frac{2\langle\mathcal{R}\rangle_{\mathcal{D}_i} a_{\mathcal{D}}^n}{3(n+6)H_{\mathcal{D}}^2} . \quad (2.17)$$

Furthermore, one can easily obtain

$$H_{\mathcal{D}}^2(a_{\mathcal{D}}) = H_{\mathcal{D}_0}^2(\Omega_m^{\mathcal{D}_0} a_{\mathcal{D}}^{-3} + \Omega_X^{\mathcal{D}_0} a_{\mathcal{D}}^n) , \quad (2.18)$$

where \mathcal{D}_0 denotes the domain at present time, and $a_{\mathcal{D}_0} = 1$ from now on.

In comparison with the deceleration parameter q in standard cosmology, an effective volume deceleration parameter $q^{\mathcal{D}}$ is interpreted as

$$q^{\mathcal{D}} = -\frac{\ddot{a}_{\mathcal{D}}}{a_{\mathcal{D}}} \frac{1}{H_{\mathcal{D}}^2} = \frac{1}{2}\Omega_m^{\mathcal{D}} + 2\Omega_{\mathcal{Q}}^{\mathcal{D}} - \Omega_\Lambda^{\mathcal{D}} . \quad (2.19)$$

3 Effective geometry

3.1 The template metric

Larena et al. [1] proposes the template metric (space-time metric) as follows,

$${}^4g^{\mathcal{D}} = -dt^2 + L_{H_0}^2 a_{\mathcal{D}}^2 \gamma_{ij}^{\mathcal{D}} dX^i \otimes dX^j , \quad (3.1)$$

where $a_{\mathcal{D}_0} L_{H_0} = 1/H_{\mathcal{D}_0}$ is introduced as the size of the horizon at present time, so that the coordinate distance is dimensionless, and the domain-dependent *effective 3-metric* reads

$$\gamma_{ij}^{\mathcal{D}} dX^i \otimes dX^j = \left(\frac{dr^2}{1 - \kappa_{\mathcal{D}}(t)r^2} + d\Omega^2 \right) , \quad (3.2)$$

with solid angle element $d\Omega^2 = r^2(d\theta^2 + \sin^2\theta d\phi^2)$. Under their assumption, the template 3-metric is identical to the spatial part of a FLRW space-time at any given time, except for the time-dependent scalar curvature. According to their discussion, $\kappa_{\mathcal{D}}$ must be related to $\langle\mathcal{R}\rangle_{\mathcal{D}}$, then in analogy with a FLRW metric, the correlation is given by

$$\langle\mathcal{R}\rangle_{\mathcal{D}} = \frac{\kappa_{\mathcal{D}}(t) |\langle\mathcal{R}\rangle_{\mathcal{D}_0}| a_{\mathcal{D}_0}^2}{a_{\mathcal{D}}^2(t)} . \quad (3.3)$$

Notice that this template metric does not need to be a dust solution of Einstein's equations, since Einstein's field equations are satisfied locally for any space-time metric. Nevertheless, this prescription is insufficient, as $\kappa_{\mathcal{D}}$ cannot be positive in this case, which is assertive and skeptical.

3.2 Computation of Observables

The computation of effective distances along the approximate smoothed light cone associated with the travel of light is very different from general that of distances [11]. Firstly, an effective volume redshift $z_{\mathcal{D}}$ is defined as

$$1 + z_{\mathcal{D}} = \frac{(g_{\mu\nu}k^\mu u^\nu)_S}{(g_{\mu\nu}k^\mu u^\nu)_O}, \quad (3.4)$$

where the O and the S represent the evaluation of the quantities at the observer and source, respectively, $g_{\mu\nu}$ is the template effective metric (29), u^μ is the 4-velocity of the matter content ($u^\mu u_\mu = -1$) with respect to comoving reference, and k^μ is the wave vector of a light ray that travels from the source S to the observer O ($k^\mu k_\mu = 1$). Normalizing the wave vector to get $(k^\mu u_\mu)_O = -1$ and defining the scaled vector $\hat{k}^\mu = a_{\mathcal{D}}^2 k^\mu$, one can obtain the following relation

$$1 + z_{\mathcal{D}} = \left(a_{\mathcal{D}}^{-1} \hat{k}^0 \right)_S, \quad (3.5)$$

where \hat{k}^0 obeys the null geodesics equation $\hat{k}^\mu \nabla_\mu \hat{k}^\nu = 0$, which leads to

$$\frac{1}{\hat{k}^0} \frac{d\hat{k}^0}{da_{\mathcal{D}}} = - \frac{r^2(a_{\mathcal{D}})}{2(1 - \kappa_{\mathcal{D}}(a_{\mathcal{D}})r^2(a_{\mathcal{D}}))} \frac{d\kappa_{\mathcal{D}}(a_{\mathcal{D}})}{da_{\mathcal{D}}}. \quad (3.6)$$

As light travels along null geodesic, we have

$$\frac{dr}{da_{\mathcal{D}}} = - \frac{H_{\mathcal{D}_0}}{a_{\mathcal{D}}^2 H_{\mathcal{D}}(a_{\mathcal{D}})} \sqrt{1 - \kappa_{\mathcal{D}}(a_{\mathcal{D}})r^2}; r(1) = 0, \quad (3.7)$$

which is slightly different from Eq. (30) of [1], since what they have chosen $r(0) = 0$ is actually $r(a_{\mathcal{D}_0} = 1) = 0$. By solving Eq. (3.7) one can get the coordinate distance $\bar{r}(a_{\mathcal{D}})$, and then substitutes it into Eq. (3.6) to find the relation between $z_{\mathcal{D}}$ and $a_{\mathcal{D}}$. Combining equations in Section 3 and Section 2, one can obtain

$$\kappa_{\mathcal{D}}(a_{\mathcal{D}}) = - \frac{(n+6)\Omega_X^{\mathcal{D}_0} a_{\mathcal{D}}^{n+2}}{|(n+6)\Omega_X^{\mathcal{D}_0}|}, \quad (3.8)$$

$$\frac{dr}{da_{\mathcal{D}}} = - \sqrt{\frac{1 - \kappa_{\mathcal{D}}(a_{\mathcal{D}})r^2}{\Omega_m^{\mathcal{D}_0} a_{\mathcal{D}} + \Omega_X^{\mathcal{D}_0} a_{\mathcal{D}}^{n+4}}}; \quad r(1) = 0. \quad (3.9)$$

When Larena et al. [1] substituted their Eq. (39) into Eq. (30), they missed one element $a_{\mathcal{D}}^{-2}$ and the negative sign, even though they used the right one as our Eq. (3.9). To check that out, we repeat the process of Larena's work, and find out a deviation, as shown in Fig. 1. Panel (a) and panel (d) of our Fig. 1 are identical with Larena's, and although their panels (b) and (c) have same evolutionary trends, our initial point of $z_{\text{FLRW}}/z_{\mathcal{D}}$ is around 1.86, which is obviously different from theirs around 2.63. Since panel (c) and panel (d) are obtained with the same method and just different equations, we remain skeptical about their results.

In dark energy context, a constant equation of state w is correlated with the component n as $w^{\mathcal{D}} = -(n+3)/3$. However, as for the time-dependent curvature of the backreaction model, due to [9], the overall 'cosmic equation of state' $w_{\text{eff}}^{\mathcal{D}}$ is given by

$$w_{\text{eff}}^{\mathcal{D}} = w_{\Phi}^{\mathcal{D}}(1 - \Omega_m^{\mathcal{D}}), \quad (3.10)$$

where $w_{\Phi}^{\mathcal{D}}$, the constant equation of state for the morphon field, represents the effect of the averaged geometrical degrees of freedom.

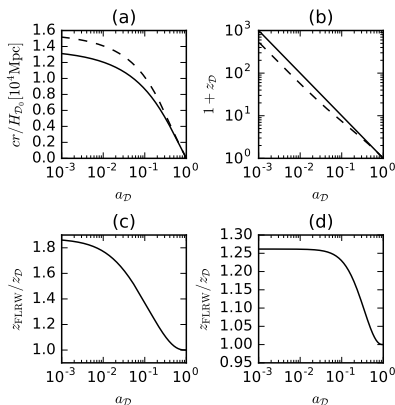


Figure 1. The evolutions of the coordinate distance $cr/H_{\mathcal{D}_0}$ (panel (a)), the redshift (panel (b)) and the ratio between the FLRW redshift to the effective redshift, $1/(a_{\mathcal{D}}(1+z_{\mathcal{D}}))$, in the averaged model as function of the effective scale factor $z_{\mathcal{D}}$ with $n = -1$, $\Omega_m^{\mathcal{D}_0} = 0.3$, $H_{\mathcal{D}_0} = 70$ km/s/Mpc (dashed line). The flat FLRW model with same parameters are the solid lines shown in panels (a) and (b), respectively. Panel (d) represents $1/(a_{\mathcal{D}}(1+z_{\mathcal{D}}))$ for Larena’s best-fit averaged model with $n = 0.12$, $\Omega_m^{\mathcal{D}_0} = 0.38$, $H_{\mathcal{D}_0} = 78.54$ km/s/Mpc.

4 Constraints with OHD

4.1 The flat FLRW model

In flat FLRW model, one can have

$$1 + z_{\mathcal{D}} = \frac{a_{\mathcal{D}_0}}{a_{\mathcal{D}}}, \quad (4.1)$$

where $z_{\mathcal{D}}$, $a_{\mathcal{D}_0}$ and $a_{\mathcal{D}}$ are assumed to be identical to z , a_0 and a , respectively. As a result, Eq. (2.18) becomes

$$H_{\mathcal{D}}^2(z_{\mathcal{D}}) = H_{\mathcal{D}_0}^2 [\Omega_m^{\mathcal{D}_0} (1 + z_{\mathcal{D}})^3 + \Omega_X^{\mathcal{D}_0} (1 + z_{\mathcal{D}})^{-n}], \quad (4.2)$$

where $\Omega_X^{\mathcal{D}_0} = 1 - \Omega_m^{\mathcal{D}_0}$, and the unknown parameters are n , $\Omega_m^{\mathcal{D}_0}$, and $H_{\mathcal{D}_0}$. We consider the prior distributions of these parameters to be all uniform distributions, and with a range of n , $\Omega_m^{\mathcal{D}_0}$, $H_{\mathcal{D}_0}$ from -3 to 3, 0.0 to 0.7, and 50.0 to 90.0, respectively. The constraints on $(n, \Omega_m^{\mathcal{D}_0})$ can be obtained by minimizing $\chi_H^2(n, \Omega_m^{\mathcal{D}_0}, H_{\mathcal{D}_0})$,

$$\chi_H^2(n, \Omega_m^{\mathcal{D}_0}, H_{\mathcal{D}_0}) = \sum_i \frac{[H_{\text{obs}}(z_i) - H_{\text{th}}(z_i, H_{\mathcal{D}_0}, n, \Omega_m^{\mathcal{D}_0})]^2}{\sigma_{H_i}^2}. \quad (4.3)$$

Here we assume that each measurement in $\{H_{\text{obs}}(z_i)\}$ is independent. However, we note that the covariance matrix of data is not necessarily diagonal, as discussed in [12], and if not, the case will become complicated and should be treated by means of the method mentioned by [12]. Despite that, if interested in the constraint of n and $\Omega_m^{\mathcal{D}_0}$, one could marginalize $H_{\mathcal{D}_0}$ to obtain the probability distribution function of n and $\Omega_m^{\mathcal{D}_0}$, i.e., the likelihood function is

$$\mathcal{L}(n, \Omega_m^{\mathcal{D}_0}) = \int dH_{\mathcal{D}_0} P(H_{\mathcal{D}_0}) e^{-\chi_H^2(n, \Omega_m^{\mathcal{D}_0}, H_{\mathcal{D}_0})/2}, \quad (4.4)$$

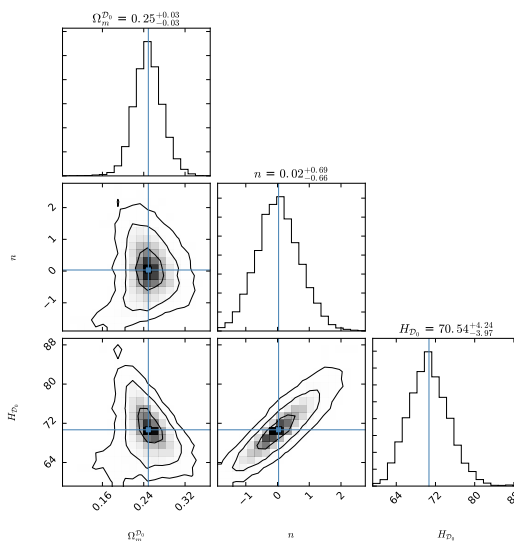


Figure 2. The 1σ , 2σ and 3σ confidence regions of the effective parameters n , $\Omega_m^{\mathcal{D}_0}$, and $H_{\mathcal{D}_0}$ for the backreaction model, along with their own probability density function.

where $P(H_{\mathcal{D}_0})$ is the prior distribution function for the present effective volume Hubble constant. Table 1 shows all 38 available OHD and reference therein, which includes data obtained by both the differential galactic ages method and the radial Baryon Acoustic Oscillation (BAO) method.

The confidence regions are demonstrated in Fig. 2. As shown in the figures, the best fits are $\Omega_m^{\mathcal{D}_0} = 0.25^{+0.03}_{-0.03}$, $n = 0.02^{+0.69}_{-0.66}$, and $H_{\mathcal{D}_0} = 70.54^{+4.24}_{-3.97}$ km/s/Mpc. As opposed to the Fig. 2 of [1], the direction of the contour ($n, \Omega_m^{\mathcal{D}_0}$) is different in our Fig. 2. In this paper, the best-fit values of $\Omega_m^{\mathcal{D}_0} = 0.25$ and $n = 0.03$, while in [1], they were given by $\Omega_m^{\mathcal{D}_0} = 0.26$ and $n = 0.24$ for the flat FLRW model. The best-fits of $\Omega_m^{\mathcal{D}_0}$ are alike, however, the values of n have nothing in common. The reason of which could be the lack of precision caused by the insufficient amount of OHD. Nevertheless, as for best-fit of $\Omega_m^{\mathcal{D}_0}$, in comparison with [26] with $\Omega_m = 0.263^{+0.042}_{-0.042}(1\sigma \text{ stat})^{+0.032}_{-0.032}(\text{sys})$ for a flat Λ CDM model, and [2] with $\Omega_m^{\text{flat}} = 0.28^{+0.09}_{-0.08}(1\sigma \text{ stat})^{+0.05}_{-0.04}(\text{sys})$ for a flat cosmology, the backreaction model along with FLRW metric seems reasonable in this sense.

Evolution of $\kappa_{\mathcal{D}}(z)$ and the dimensionless averaged cosmological parameters are illustrated in Fig. 3 (c) and (d), respectively, with the best fits of $n = 0.03$, and $\Omega_m^{\mathcal{D}_0} = 0.25$. It obviously evolves from 0 to -1, which is biased. Furthermore, we substitute the best-fit values into the effective volume deceleration parameter $q^{\mathcal{D}}$

$$\begin{aligned}
 q^{\mathcal{D}} &= -\frac{n+2}{2} + \frac{n+3}{2}\Omega_m^{\mathcal{D}} \\
 &= -\frac{n+2}{2} + \frac{(n+3)\Omega_m^{\mathcal{D}_0}}{2[\Omega_m^{\mathcal{D}_0} + (1-\Omega_m^{\mathcal{D}_0})(1+z)^{-(n+3)}]}.
 \end{aligned} \tag{4.5}$$

Consequently, we plot this relation into the $q^{\mathcal{D}}-z$ figure. Fig. 3 (a) illustrates how the volume deceleration parameter $q^{\mathcal{D}}$ evolves with redshift z with best-fit values of n and $\Omega_m^{\mathcal{D}_0}$. The transition redshift z_t from a deceleration to accelerated phase is approximately 0.815, and the present value of the volume deceleration parameter $q^{\mathcal{D}_0}$ is about -0.636. While

z	$H(z)$	Method	Ref.
0.0708	69.0 ± 19.68	I	Zhang et al. (2014)-[13]
0.09	69.0 ± 12.0	I	Jimenez et al. (2003)-[14]
0.12	68.6 ± 26.2	I	Zhang et al. (2014)-[13]
0.17	83.0 ± 8.0	I	Simon et al. (2005)-[15]
0.179	75.0 ± 4.0	I	Moresco et al. (2012)-[16]
0.199	75.0 ± 5.0	I	Moresco et al. (2012)-[16]
0.20	72.9 ± 29.6	I	Zhang et al. (2014)-[13]
0.240	79.69 ± 2.65	II	Gaztañaga et al. (2009)-[17]
0.27	77.0 ± 14.0	I	Simon et al. (2005)-[15]
0.28	88.8 ± 36.6	I	Zhang et al. (2014)-[13]
0.35	84.4 ± 7.0	II	Xu et al. (2013)-[18]
0.352	83.0 ± 14.0	I	Moresco et al. (2012)-[16]
0.3802	83.0 ± 13.5	I	Moresco et al. (2016)-[19]
0.4	95 ± 17.0	I	Simon et al. (2005)-[15]
0.4004	77.0 ± 10.2	I	Moresco et al. (2016)-[19]
0.4247	87.1 ± 11.2	I	Moresco et al. (2016)-[19]
0.43	86.45 ± 3.68	II	Gaztanaga et al. (2009)-[17]
0.44	82.6 ± 7.8	II	Blake et al. (2012)-[20]
0.4497	92.8 ± 12.9	I	Moresco et al. (2016)-[19]
0.4783	80.9 ± 9.0	I	Moresco et al. (2016)-[19]
0.48	97.0 ± 62.0	I	Stern et al. (2010)-[21]
0.57	92.4 ± 4.5	II	Samushia et al. (2013)-[22]
0.593	104.0 ± 13.0	I	Moresco et al. (2012)-[16]
0.6	87.9 ± 6.1	II	Blake et al. (2012)-[20]
0.68	92.0 ± 8.0	I	Moresco et al. (2012)-[16]
0.73	97.3 ± 7.0	II	Blake et al. (2012)-[20]
0.781	105.0 ± 12.0	I	Moresco et al. (2012)-[16]
0.875	125.0 ± 17.0	I	Moresco et al. (2012)-[16]
0.88	90.0 ± 40.0	I	Stern et al. (2010)-[21]
0.9	117.0 ± 23.0	I	Simon et al. (2005)-[15]
1.037	154.0 ± 20.0	I	Moresco et al. (2012)-[16]
1.3	168.0 ± 17.0	I	Simon et al. (2005)-[15]
1.363	160.0 ± 33.6	I	Moresco (2015)-[23]
1.43	177.0 ± 18.0	I	Simon et al. (2005)-[15]
1.53	140.0 ± 14.0	I	Simon et al. (2005)-[15]
1.75	202.0 ± 40.0	I	Simon et al. (2005)-[15]
1.965	186.5 ± 50.4	I	Moresco (2015)-[23]
2.34	222.0 ± 7.0	II	Delubac et al. (2015)-[24]

Table 1. The current available OHD dataset [25]. The method I is the differential galactic ages method, and II represents the radial Baryon Acoustic Oscillation (BAO) method. $H(z)$ is in units of km/s/Mpc here.

the transition value in [27] is constrained to be $z_t = 0.46 \pm 0.13$, and the transition value in [28] is $z_t = 0.68^{+0.10}_{-0.09}$ corresponding to the present value of the deceleration parameter $q_0 = -0.48^{+0.11}_{-0.14}$ with flat prior on H_0 , we find our transition redshift and q^{D_0} are both higher

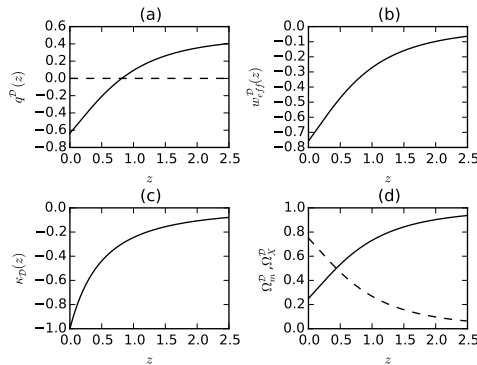


Figure 3. (a) The evolution of $q^{\mathcal{D}}$ with best-fit values of $n = 0.03$, and $\Omega_m^{\mathcal{D}0} = 0.25$; (b) The evolution of $w_{\text{eff}}^{\mathcal{D}}(z)$ with the same best-fit values as in (a); (c) The relation between $\kappa_{\mathcal{D}}(z)$ and z with the same best-fit values as in (a); (d) The evolution of $\Omega_m^{\mathcal{D}}$ (solid line) and $\Omega_X^{\mathcal{D}}$ (dashed line) with the same best fits as in (a).

than them. Of course, since the flat FLRW relation does not fit averaged model, the result is foreseeable. The overall cosmic equation of state $w_{\text{eff}}^{\mathcal{D}}$ is given by

$$\begin{aligned} w_{\text{eff}}^{\mathcal{D}} &= w_{\Phi}^{\mathcal{D}}(1 - \Omega_m^{\mathcal{D}}) \\ &= w_{\Phi}^{\mathcal{D}} \left\{ 1 - \frac{\Omega_m^{\mathcal{D}0}}{[\Omega_m^{\mathcal{D}0} + (1 - \Omega_m^{\mathcal{D}0})(1+z)^{-(n+3)}]} \right\} \end{aligned} \quad (4.6)$$

With the best-fit values of n and $\Omega_m^{\mathcal{D}0}$, we can also plot the $w_{\text{eff}}^{\mathcal{D}}-z$ figure as shown in Fig. 3 (b). The present value $w_{\text{eff}}^{\mathcal{D}0}$ is approximately -0.758.

4.2 The template metric model

In the template metric context, as mentioned above, one cannot directly constrain parameters with the expression of Eq. (2.18). However, by using Runge-Kutta method to solve Eq. (3.9), Eq. (3.6) and subsequently Eq. (3.5) with certain values of n and $\Omega_m^{\mathcal{D}0}$, one can form a one-to-one correspondence of $a_{\mathcal{D}}$ and $z_{\mathcal{D}}$, and then the constraint on parameters of Eq. (2.18) with OHD could be performed. Thus, one can rewrite Eq. (2.18) as follows

$$\begin{aligned} H_{\mathcal{D}}(a_{\mathcal{D}}) &= H_{\mathcal{D}0} \sqrt{\Omega_m^{\mathcal{D}0} a_{\mathcal{D}}^{-3} + (1 - \Omega_m^{\mathcal{D}0}) a_{\mathcal{D}}^n} \\ \Leftrightarrow H_{\mathcal{D}}(z_{\mathcal{D}}) &= H_{\mathcal{D}0} E(z_{\mathcal{D}}, n, \Omega_m^{\mathcal{D}0}) . \end{aligned} \quad (4.7)$$

After marginalizing the likelihood function over $H_{\mathcal{D}0}$, one can obtain parameter constraints in $(n, \Omega_m^{\mathcal{D}0})$ subspace. As Ma et. al. [10] stated, with top-hat prior of $H_{\mathcal{D}0}$ over the interval $[x, y]$, the posterior probability density function (PDF) of parameters given the dataset $\{H_i\}$ by Bayes' theorem reads

$$P(n, \Omega_m^{\mathcal{D}0} | \{H_i\}) = \frac{U(x, C, D) - U(y, C, D)}{\sqrt{C}} \exp\left(\frac{D^2}{C}\right) \quad (4.8)$$

where

$$C = \sum_i \frac{E^2(z_i; n, \Omega_m^{\mathcal{D}0})}{2\sigma_i^2}, \quad D = \sum_i \frac{E(z_i; n, \Omega_m^{\mathcal{D}0}) H_i}{2\sigma_i^2},$$

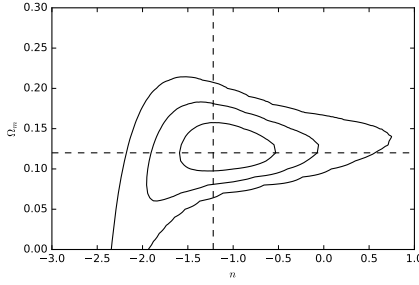


Figure 4. The 1σ , 2σ and 3σ confidence regions of the effective parameters n , $\Omega_m^{\mathcal{D}_0}$, marginalizing $H_{\mathcal{D}_0}$ over the interval $[50, 90]$. Where the best-fits are $n = -1.22$, and $\Omega_m^{\mathcal{D}_0} = 0.12$.

and

$$U(x, \alpha, \beta) = \text{erf}\left(\frac{\beta - x\alpha}{\sqrt{\alpha}}\right),$$

where $x = 50.0$, $y = 90.0$, and erf represents the error function. In the process, we utilize so called mesh-grid method to scan spots of $(n, \Omega_m^{\mathcal{D}_0})$ subspace with the range of n , and $\Omega_m^{\mathcal{D}_0}$ to be $[-2, 4]$ and $[0.0, 0.7]$, respectively. Eventually, as shown in Fig. 4, we attain the constraints with $n = -1.22^{+0.68}_{-0.40}$, and $\Omega_m^{\mathcal{D}_0} = 0.12^{+0.04}_{-0.02}$. Apparently, our results are quite different from Larena's results with $\Omega_m^{\mathcal{D}_0} = 0.397$ and $n = 0.5$ for averaged model. Since these are all based on the power law ansatz of $a_{\mathcal{D}}$, it leaves the issue to be the wrong prescription of $\kappa_{\mathcal{D}}$ (power law ansatz), the chosen prior of $H_{\mathcal{D}_0}$, or the lack of amount for OHD.

To test the probability of the second reason, we select three different Gaussian prior distributions of $H_{\mathcal{D}_0}$ to evaluate the results. At this circumstance, as described in [10], the posterior PDF of parameters becomes

$$P(n, \Omega_m^{\mathcal{D}_0} | \{H_i\}) = \frac{1}{\sqrt{A}} [\text{erf}\left(\frac{B}{\sqrt{A}}\right) + 1] \exp\left(\frac{B^2}{A}\right), \quad (4.9)$$

where

$$A = \frac{1}{2\sigma_H^2} \sum_i \frac{E^2(z_i; n, \Omega_m^{\mathcal{D}_0})}{2\sigma_i^2},$$

$$B = \frac{\mu_H}{2\sigma_H^2} \sum_i \frac{E^2(z_i; n, \Omega_m^{\mathcal{D}_0}) H_i}{2\sigma_i^2},$$

where μ_H and σ_H^2 denote prior expectation and deviation of $H_{\mathcal{D}_0}$, respectively. First, we make use of $H_{\mathcal{D}_0} = 69.32 \pm 0.80$ km/s/Mpc [29] to obtain the constraints. As a result, Fig. 5 illustrates the confidence regions with 1σ constraints $n = -0.88^{+0.26}_{-0.23}$, and $\Omega_m^{\mathcal{D}_0} = 0.12^{+0.03}_{-0.03}$. Second, as shown in Fig. 6, we acquire the constraints $n = -1.04^{+0.27}_{-0.31}$ and $\Omega_m^{\mathcal{D}_0} = 0.13^{+0.02}_{-0.03}$ with $H_{\mathcal{D}_0} = 67.3 \pm 1.2$ km/s/Mpc [30]. Last, we attain the constraints with Gaussian prior of $H_{\mathcal{D}_0} = 73.24 \pm 1.74$ km/s/Mpc [31], as depicted in Fig. 7, $n = -0.58^{+0.36}_{-0.34}$ and $\Omega_m^{\mathcal{D}_0} = 0.12^{+0.02}_{-0.03}$. As a result, we find out that although three Gaussian priors lead to different best-fit values of n , the best-fits of $\Omega_m^{\mathcal{D}_0}$ are compatible with the result of top-hat prior. Therefore, the prior issue can be excluded. Since the same set of data shared by FLRW case result in a reasonable conclusion, the lack of amount for OHD can also be neglected. Therefore, the power law ansatz should not be applied on $\kappa_{\mathcal{D}}$, and some other scenarios should be introduced.

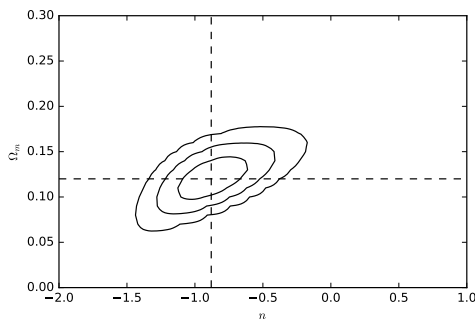


Figure 5. The 1σ , 2σ and 3σ confidence regions of the effective parameters n , $\Omega_m^{\mathcal{D}_0}$ with Gaussian prior of $H_{\mathcal{D}_0} = 69.32 \pm 0.80$ km/s/Mpc. Here the best-fits are $n = -0.88$, and $\Omega_m^{\mathcal{D}_0} = 0.12$.

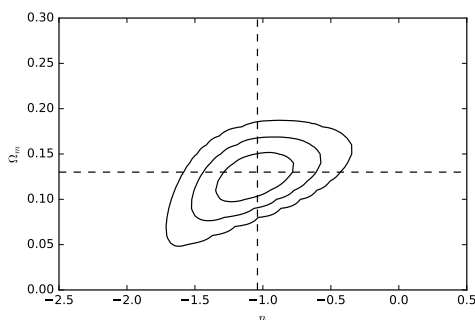


Figure 6. Same as Fig. 5, but with Gaussian prior of $H_{\mathcal{D}_0} = 67.3 \pm 1.2$ km/s/Mpc. Here the best-fits are $n = -1.04$, and $\Omega_m^{\mathcal{D}_0} = 0.13$.

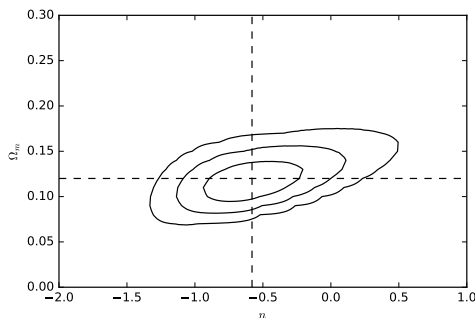


Figure 7. Same as Fig. 5, but with Gaussian prior of $H_{\mathcal{D}_0} = 73.24 \pm 1.74$ km/s/Mpc. Here the best-fits are $n = -0.58$, and $\Omega_m^{\mathcal{D}_0} = 0.12$.

Our results indicate that it demands lower values of $\Omega_m^{\mathcal{D}_0}$ for the models to be compatible with data, which means that on the contrary with Larena's conclusion, a larger amount of backreaction is required to account for effective geometry. As mentioned in [1], a dark energy model in FLRW context with $n = -1$ is compatible with the data at 1σ for $\Omega_m^{\mathcal{D}_0} \sim 0.1$, and as calculated in [32] and [33], the leading perturbative model ($n = -1$) is marginally at 1σ for $\Omega_m^{\mathcal{D}_0} \sim 0.3$. As expected, purely perturbative estimate of backreaction could not provide

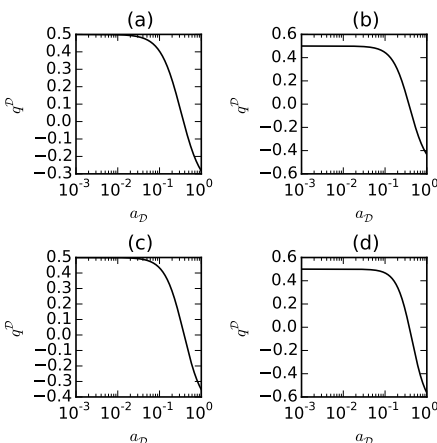


Figure 8. The evolutions of $q^{\mathcal{D}}$ against effective scale factor $a_{\mathcal{D}}$ with best-fit values of (a) $n = -1.22$, $\Omega_m^{\mathcal{D}0} = 0.12$, (b) $n = -0.88$, $\Omega_m^{\mathcal{D}0} = 0.12$, (c) $n = -1.04$, $\Omega_m^{\mathcal{D}0} = 0.13$, and (d) $n = -0.58$, $\Omega_m^{\mathcal{D}0} = 0.12$, respectively.

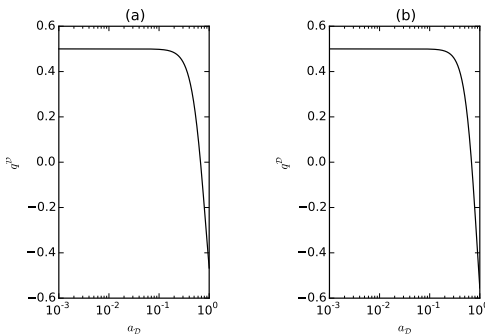


Figure 9. Evolutions of $q^{\mathcal{D}}$ against effective scale factor $a_{\mathcal{D}}$ with best-fit values of (a) $n = 0.12$, $\Omega_m^{\mathcal{D}0} = 0.38$, (b) $n = 0.5$, $\Omega_m^{\mathcal{D}0} = 0.397$.

sufficient geometrical effect to account for observations. What is not expected is that the values of $\Omega_m^{\mathcal{D}0}$ is higher or lower compared to the standard dark energy models with a FLRW geometry. The following subsection explores the effective deceleration parameter $q^{\mathcal{D}}$ evolves against $a_{\mathcal{D}}$ in many cases, in order to pinpoint the hinge of the issue.

4.3 Testing the effective deceleration parameter

Fig. 8 shows the evolutions of $q^{\mathcal{D}}$ against effective scale factor $a_{\mathcal{D}}$ with our best-fit values. One can gain the information that in each case $q^{\mathcal{D}}$ tends to 0.5 as $a_{\mathcal{D}}$ to be smaller, and they all have sufficient backreaction to meet the observations, at least in this perspective. This indicate that the observational data do not disfavour the constraints. However, we also illustrate the same evolutions by using the absolute and the marginalized best-fits of Larena et. al., as shown in Fig. 9, and surprisingly find out the similar conclusion. This further favours our doubt about the power law prescription of $\kappa_{\mathcal{D}}$.

5 Conclusions and discussions

In this paper, we combine backreaction model of dust cosmology with both FLRW metric and smoothed template metric to constrain parameters with observational Hubble parameter data (OHD). The purpose of which is to explore the generic properties of a backreaction model to explain the observations of the Universe. Unlike [34], first, in the FLRW model, we constrain two of three parameters with MCMC method by marginalizing the likelihood function over the rest one parameter, and obtain the best fits as $\Omega_m^{\mathcal{D}_0} = 0.25_{-0.03}^{+0.03}$, $n = 0.02_{-0.66}^{+0.69}$, and $H_{\mathcal{D}_0} = 70.54_{-3.97}^{+4.24}$ km/s/Mpc. At this best-fit model, we employ the best-fit values of n and $\Omega_m^{\mathcal{D}_0}$ to study the evolutions of $q^{\mathcal{D}}$, $w_{\text{eff}}^{\mathcal{D}}$, $\kappa_{\mathcal{D}}$, and effective density parameters. The results compared with other models are slightly biased, which is normal as for the inconsistency between FLRW geometry and averaged model.

Second, with template metric and the specific method of how to compute the observables along null geodesic, we choose a top-hat prior, i.e., uniform distribution of $H_{\mathcal{D}_0}$ to be marginalized, in order to attain the posterior PDF of parameters. By making use of classical mesh-grid method, we programme to scan point-by-point in the subspace of $(n, \Omega_m^{\mathcal{D}_0})$ to obtain the probability of every point, and subsequently plot the contours. By means of that, we obtain the best-fit values, which are $n = -1.22_{-0.41}^{+0.68}$ and $\Omega_m^{\mathcal{D}_0} = 0.12_{-0.02}^{+0.04}$. The value of $\Omega_m^{\mathcal{D}_0}$ is considerably small in comparison with Larena's. Our results indicate that it demands lower values of $\Omega_m^{\mathcal{D}_0}$ for the models to be compatible with data, which means that on the contrary with Larena's conclusion, a larger amount of backreaction is required to account for effective geometry. Since these are all based on the power law ansatz of $a_{\mathcal{D}}$, it leaves the issue to be the wrong prescription of $\kappa_{\mathcal{D}}$ (power law ansatz), the chosen prior of $H_{\mathcal{D}_0}$, or the lack of amount for OHD. Since the same set of data shared by FLRW case result in a reasonable conclusion, the lack of amount for OHD can be neglected in a way. To test the probability of the second reason, we select three different Gaussian prior distributions of $H_{\mathcal{D}_0}$ to evaluate the results. Subsequently, we obtain three sets of best-fits: $n = -0.88_{-0.23}^{+0.26}$, and $\Omega_m^{\mathcal{D}_0} = 0.12_{-0.03}^{+0.03}$, corresponding to $H_{\mathcal{D}_0} = 69.32 \pm 0.80$ km/s/Mpc [29]; $n = -1.04_{-0.31}^{+0.27}$, and $\Omega_m^{\mathcal{D}_0} = 0.13_{-0.03}^{+0.02}$ with $H_{\mathcal{D}_0} = 67.3 \pm 1.2$ km/s/Mpc [30]; $n = -0.58_{-0.34}^{+0.36}$, and $\Omega_m^{\mathcal{D}_0} = 0.12_{-0.03}^{+0.02}$, related to $H_{\mathcal{D}_0} = 73.24 \pm 1.74$ km/s/Mpc [31]. As a result, we find out that although three Gaussian priors lead to different best-fit values of n , the best-fits of $\Omega_m^{\mathcal{D}_0}$ are still compatible with the result of top-hat prior. Therefore, the prior issue can be excluded. Since the same set of data shared by FLRW case result in a reasonable conclusion, the lack of amount for OHD can also be neglected. Eventually, we believe that the power law ansatz should not be applied on $\kappa_{\mathcal{D}}$, and some other scenarios should be introduced.

In order to further pinpoint the hinge of the issue, we explore the evolutions of $q^{\mathcal{D}}$ against effective scale factor $a_{\mathcal{D}}$ with best-fit values of both us and Larena et. al. It turns out that both results are similar in the tendency of the evolutions. In other words, despite of the constraints of the effective parameters, there are not much differences, which leaves both the constraints less meaningful. That just prove our point that one must remain skeptical on the power law ansatz of $\kappa_{\mathcal{D}}$ and consider other options.

Acknowledgments

We are grateful to Yu Liu for useful discussion. This work was supported by the National Science Foundation of China (Grants No. 11573006, 11528306), the Ministry of Science and Technology National Basic Science program (project 973) under grant No. 2012CB821804.

References

- [1] J. Larena, J.-M. Alimi, T. Buchert, M. Kunz and P.-S. Corasaniti, *Testing backreaction effects with observations*, *Phys. Rev. D - Part. Fields, Gravit. Cosmol.* **79** (2009) 1–28, [0808.1161].
- [2] S. Perlmutter, G. Aldering and G. Goldhaber, et al., *Measurements of Ω and Λ from 42 High-Redshift Supernovae*, *Astrophys. J.* **517** (1999) 565–586, [9812133].
- [3] A. G. Riess, A. V. Filippenko and P. Challis, et al., *Observational Evidence from Supernovae for an Accelerating Universe and a Cosmological Constant*, *Astron. J.* **116** (1998) 1009–1038, [9805201].
- [4] E. J. Copeland, M. Sami and S. Tsujikawa, *Dynamics of dark energy*, *International Journal of Modern Physics D* **15** (2006) 1753–1935, [0603057].
- [5] V. Gorini, A. Y. Kamenshchik, U. Moschella, O. F. Piattella and A. A. Starobinsky, *More about the Tolman-Oppenheimer-Volkoff equations for the generalized Chaplygin gas*, *Phys. Rev. D - Part. Fields, Gravit. Cosmol.* **80** (2009) 104038, [0909.0866].
- [6] S. Räsänen, *Dark energy from backreaction*, *J. Cosmol. Astropart. Phys.* **2** (2004) 003–003, [0311257].
- [7] E. W. Kolb, S. Matarrese and A. Riotto, *On cosmic acceleration without dark energy*, *New J. Phys.* **8** (2006) 322, [0506534].
- [8] T. Buchert, *On average properties of inhomogeneous fluids in general relativity I: dust cosmologies*, *Gen. Relativ. Gravit.* **32** (2000) 105–126, [9906015].
- [9] T. Buchert, J. Larena and J.-M. Alimi, *Correspondence between kinematical backreaction and scalar field cosmologies—the ‘morphon field’*, *Classical and Quantum Gravity* **23** (Nov., 2006) 6379–6408, [gr-qc/0606020].
- [10] C. Ma and T.-J. Zhang, *Power of Observational Hubble Parameter Data: A Figure of Merit Exploration*, *Astrophys. J.* **730** (Apr., 2011) 74, [1007.3787].
- [11] C. Bonvin, R. Durrer and M. A. Gasparini, *Fluctuations of the luminosity distance*, *Phys. Rev. D - Part. Fields, Gravit. Cosmol.* **73** (2006) , [0511183].
- [12] H.-R. Yu, S. Yuan and T.-J. Zhang, *Nonparametric reconstruction of dynamical dark energy via observational Hubble parameter data*, *Phys. Rev. D* **88** (Nov., 2013) 103528, [1310.0870].
- [13] C. Zhang, H. Zhang, S. Yuan, S. Liu, T.-J. Zhang and Y.-C. Sun, *Four new observational $H(z)$ data from luminous red galaxies in the Sloan Digital Sky Survey data release seven*, *Research in Astronomy and Astrophysics* **14** (Oct., 2014) 1221–1233, [1207.4541].
- [14] R. Jimenez, L. Verde, T. Treu and D. Stern, *Constraints on the equation of state of dark energy and the Hubble constant from stellar ages and the CMB*, *Astrophys. J.* **593** (feb, 2003) 622–629, [0302560].
- [15] J. Simon, L. Verde and R. Jimenez, *Constraints on the redshift dependence of the dark energy potential*, *Phys. Rev. D - Part. Fields, Gravit. Cosmol.* **71** (2005) 123001, [0412269].
- [16] M. Moresco, L. Verde, L. Pozzetti, R. Jimenez and A. Cimatti, *New constraints on cosmological parameters and neutrino properties using the expansion rate of the Universe to $z \sim 1.75$* , *J. Cosmol. Astropart. Phys.* (2012) 53, [1201.6658].
- [17] E. Gaztañaga, A. Cabré and L. Hui, *Clustering of Luminous Red Galaxies IV: Baryon Acoustic Peak in the Line-of-Sight Direction and a Direct Measurement of $H(z)$* , 0807.3551.
- [18] X. Xu, A. J. Cuesta, N. Padmanabhan, D. J. Eisenstein and C. K. McBride, *Measuring D_A and H at $z = 0.35$ from the SDSS DR7 LRGs using baryon acoustic oscillations*, *Mon. Not. R. Astron. Soc.* **431** (2013) 2834–2860, [1206.6732].

- [19] M. Moresco, L. Pozzetti and A. Cimatti et al., *A 6% measurement of the Hubble parameter at $z \sim 0.45$: direct evidence of the epoch of cosmic re-acceleration*, *Journal of Cosmology and Astroparticle Physics* **5** (May, 2016) 014, [[1601.01701](#)].
- [20] C. Blake, S. Brough and M. Colless, et al., *The WiggleZ Dark Energy Survey: Joint measurements of the expansion and growth history at $z < 1$* , *Mon. Not. R. Astron. Soc.* **425** (2012) 405–414, [[1204.3674](#)].
- [21] D. Stern, R. Jimenez and L. Verde, et al., *Cosmic chronometers: constraining the equation of state of dark energy. I: $H(z)$ measurements*, *J. Cosmol. Astropart. Phys.* **2** (2010) 8, [[0907.3149v1](#)].
- [22] L. Samushia, B. A. Reid and M. White, et al., *The clustering of galaxies in the SDSS-III DR9 baryon oscillation spectroscopic survey: Testing deviations from Λ and general relativity using anisotropic clustering of galaxies*, *Mon. Not. R. Astron. Soc.* **429** (2013) 1514–1528, [[1206.5309](#)].
- [23] M. Moresco, *Raising the bar: New constraints on the Hubble parameter with cosmic chronometers at $z \sim 2$* , *Mon. Not. R. Astron. Soc. Lett.* **450** (2015) L16–L20, [[1503.01116](#)].
- [24] T. Delubac, J. E. Bautista and N. G. Busca, et al., *Baryon Acoustic Oscillations in the Ly α forest of BOSS DR11 quasars*, *Astron. Astrophys.* **574** (2015) A59, [[1404.1801](#)].
- [25] X.-W. Duan, M. Zhou and T.-J. Zhang, *Testing consistency of general relativity with kinematic and dynamical probes*, *ArXiv e-prints* (May, 2016) , [[1605.03947](#)].
- [26] P. Astier, J. Guy and N. Regnault, et al., *The Supernova Legacy Survey: measurement of Ω_M , Ω_Λ and w from the first year data set*, *Astron. Astrophys.* **447** (2006) 31–48, [[0510447](#)].
- [27] A. G. Riess, L.-G. Strolger and J. Tonry, et al., *Type Ia Supernova Discoveries at $z > 1$ from the Hubble Space Telescope : Evidence for Past Deceleration and Constraints on Dark Energy Evolution*, *Astrophys. J.* **607** (2004) 665–687, [[0402512](#)].
- [28] M. Vargas dos Santos, R. R. R. Reis and I. Waga, *Constraining cosmic deceleration-acceleration transition with type Ia supernova, BAO/CMB and $H(z)$ data*, *J. Cosmol. Astropart. Phys.* **02** (2016) 13, [[1505.03814](#)].
- [29] C. L. Bennett, D. Larson and J. L. Weiland et. al., *Nine-year Wilkinson Microwave Anisotropy Probe (WMAP) Observations: Final Maps and Results*, *The Astrophysical Journal Supplement* **208** (Oct., 2013) 20, [[1212.5225](#)].
- [30] Planck Collaboration, P. A. R. Ade and N. Aghanim et al., *Planck 2013 results. XVI. Cosmological parameters*, *Astronomy and Astrophysics* **571** (Nov., 2014) A16, [[1303.5076](#)].
- [31] A. G. Riess, L. M. Macri and S. L. Hoffmann et. al., *A 2.4% Determination of the Local Value of the Hubble Constant*, *Astrophys. J.* **826** (July, 2016) 56, [[1604.01424](#)].
- [32] N. Li and D. J. Schwarz, *Onset of cosmological backreaction*, *Phys. Rev. D* **76** (Oct., 2007) 083011, [[gr-qc/0702043](#)].
- [33] N. Li, M. Seikel and D. J. Schwarz, *Is dark energy an effect of averaging?*, *Fortschritte der Physik* **56** (Apr., 2008) 465–474, [[0801.3420](#)].
- [34] M. Chiesa, D. Maino and E. Majerotto, *Observational tests of backreaction with recent data*, *J. Cosmol. Astropart. Phys.* (2014) 49, [[1405.7911](#)].